

Proceedings of the Korean Nuclear Society Spring Meeting

Cheju, Korea, May 2001

**Thermal Hydraulic and Structural Analysis of
Liquid Metal Target and Window**

Yong Suk Lee, Chang Hyun Chung

Seoul National University

San56-1 Shinlim-dong, Kwanak-gu

Seoul, Korea

ABSTRACT

A subcritical transmutation reactor research is in progress for treatment of spent fuel. The subcritical transmutation reactor needs target system to produce high-energy neutrons. In target system, beam window is subject to high thermal field, because it interacts with high energy proton beam. In this study, thermal-hydraulic analysis was performed to design target which cools down window effectively. Then, thermal and structural analysis of window was performed to find out dominant parameters on window structural safety and to establish base parameter values of target.

1. Introduction

Spent fuel treatment and disposal problem is one of the important issues in nuclear industry. There are many high toxic radioactive isotopes in spent fuel, so they can have serious effect on human and environment. So, a research for transmutation is in progress to transmute high radioactive isotopes into low radioactive ones. Subcritical transmutation is considered one of the appropriate method among many concepts related with transmutation. Subcritical transmutation reactor maintains fission reaction by adding neutrons produced by spallation reaction of proton beam and target. Figure 1 shows conceptual design of subcritical transmutation reactor. High energy proton beam goes through window and target, so a large amount of heat is generated.

Because research on this issue is in the beginning stage, geometry and design values of target and window has not been determined yet. In this study, thermal-hydraulic analysis of target was performed using commercial CFD code FLUENT^[1], and target was designed to enhance window cooling. Then, thermal-structural analysis of window was performed using structural analysis code ANSYS^[2]

varying design parameters to find dominant parameters on window structural safety and to establish base parameter values of target.

2. Thermal Hydraulic Analysis and Design of Liquid Metal Target

First, the target was designed an axi-symmetric device as shown in figure 2. Liquid Pb-Bi was selected for target material, so it can also be used as coolant material for window. Forced convection assumption and standard $k-\varepsilon$ turbulent model was used. FLUENT code was used in velocity and temperature calculation.

Proton beam is injected downward to window and target, with parabolic intensity distribution having diameter of 10cm as follows:

$$\phi(p/cm^2 \cdot s \cdot mA) = \frac{1.6 \times 10^{14}}{5^2} (5^2 - r^2)$$

Heat is generated by spallation reaction with proton beam and target, or window. Heat generation rate from LAHET code calculation by KAERI^[3] was applied to the target and window, and is shown in table 1. It is assumed that beam power is 1GeV, 2mA, and Pb-Bi flow rate is 0.1m³/s. Window diameter is 30cm, the external surface of the window is an hemisphere while the internal surface is an ellipsoid, so that the window thickness arises from a minimum of 1mm in the beam axis to a maximum of 3mm in the junction with the beam pipe. This is to reduce the thickness as much as possible in the zone where proton irradiation is higher. 9Cr-2WVTa ferrite-martensite steel was selected as beam window for its good mechanical and irradiation characteristics.

2.1 Effect of flow direction

First, the effect of “downward flow” and “upward flow” was compared. In downward flow, the coolant enters at first into the outer annular section. It is bended at the top region, cools down the window and exits inner circular section. In upward flow, the coolant enters inner circular section, cools the window and exits outer annular section.

Figure 3 shows the window and coolant temperature along the symmetric line of the target for downward flow and upward flow. In case of downward flow, temperature gradient happens only in the region close to the window. In the case of upward flow, the coolant temperature increases continuously by approaching the window and maximum window temperature in the window is about 57K higher than in the case of downward flow.

In case of downward flow the coolant temperature before cooling the window is about the same as the coolant temperature entering the active part. Moreover, there is a big change of coolant velocity in the central region as shown in figure 4. This indicates a strong transverse exchange of momentum and energy. In case of upward flow the coolant is heated up before cooling window, so result in a higher temperature of the window. The coolant velocity is nearly constant, except for the region near the

window as shown in figure 4. So it can be explained that the transverse exchange of momentum and energy is weak. For this reason, coolant temperature increases continuously at the central axis.

Because maximum window temperature was lower in case of downward flow, downward flow is selected for reference target cooling design.

2.2 Diffuse plate installation

In the target velocity calculation, flow stagnation zone appeared near window. Because maximum temperature appears in window center, it is important to reduce stagnation zone near window center to keep the window temperature low. To reduce stagnation zone, a diffuse plate installation was considered. Diffuse plate material is 9Cr-2WVTa steel with distributed holes as shown in figure 3. Relating to distribution of holes, diffuse plate was divided three zones with radius of 5cm, 10cm, 16cm. Porosities are assigned to 0.64, 0.42, 0.2. To increase flow velocity near window center, higher porosity was assigned in the center of diffuse plate. In this simulation, holes of on the diffuse plate are simplified by annuli. Area of annuli was set same as the area of the holes.

2.3 Effect of distance between diffuse plate and window

By varying distance between diffuse plate and window, maximum window temperature can be varied. Distance between diffuse plate and window was varied 60mm, 30mm, 15mm, 8mm and window temperature was calculated. As expected, decrease of the distance resulted in decrease of window temperature. Maximum temperature calculation results is presented in table 2. Because maximum window temperature is lowest in 8mm case, a distance of 8mm was selected for reference target design.

3. Thermal-Structural Analysis of Beam Window

In target system, maximum temperature appears in beam window. So, it is necessary to analyze window temperature elevation in various design conditions. Mechanical stress can be induced in window by these severe thermal loads and some hydrostatic pressure. So, preliminary structural as well as thermal analysis is needed for window.

Beam window temperature were analyzed varying design parameters. These design parameters are beam power, coolant flow rate, minimum window thickness. Mechanical stress of beam window were also analyzed using commercial structural analysis code ANSYS. Figure 11 represents beam window temperature distribution as an angle from beam axis, at beam power 1GeV, 2mA, coolant flow rate $0.1\text{m}^3/\text{sec}$. “Internal” means window internal surface adjacent to evacuated region, “external” means external surface of window adjacent to Pb-Bi target, “mid” means middle of internal and external surfaces. Large temperature gradient can be observed along the thickness of window. Figure 11 represents beam window hoop stress distribution as an angle from beam axis, at beam power 1GeV,

2mA, coolant flow rate $0.1\text{m}^3/\text{sec}$. Because inside the beam tube is evacuated, hydrostatic pressure difference $3\times 10^5\text{Pa}$ was assumed conservatively. As shown in figure 11 thermally-induced bending stress is generated in window by temperature gradient along the window thickness.

3.1 Effect of minimum window thickness

Window temperature and stress calculations were performed varying minimum window thickness. Beam tube thickness was fixed to 3mm in all cases. Beam power and coolant flow rate were assumed 1GeV, 2mA and $0.1\text{m}^3/\text{sec}$. Maximum window temperature and temperature gradient increased as increasing minimum window thickness, and thermal stress also increased as shown in figure 12. But decreasing window thickness results in negative impact on pressure induced window stress. In this structural calculation result, 0.7mm case was optimized case in view of total stress. But decrease of window thickness can also result in additional negative impact; corrosion, fracture, etc. Here, window minimum thickness of 1mm was chosen preliminary.

3.2 Effect of beam power

Window temperature and stress calculation, were performed varying beam power. The window temperature and stress were calculated for the case of 1GeV, 6.78mA as the reference case, which condition is beam power design value of HYPER^[3]. HYPER is subcritical transmutation reactor which is now under conceptual designing stage in KAERI. Window minimum thickness and coolant flow rate have been assumed 1mm and $0.1\text{m}^3/\text{sec}$. Maximum window temperature and temperature gradient increased as increasing accelerator beam power, and maximum von-mises stress also increased as shown in figure 13. In the figure, temperature upper limit has been set 870K regarding window corrosion problem^[3], and von-mises stress upper limit has been set 230MPa which is yield stress of 9Cr-2WTa at 870K^[4]. Only in 10mA case, window maximum temperature and stress exceeded upper limit. So, it can be concluded that the target and the window can be used in subcritical transmutation reactor (Beam power 1GeV, 6.78mA condition).

3.3 Effect of coolant flow rate

Window temperature and stress calculation were performed varying Pb-Bi coolant flow rate. Beam power and minimum window thickness were assumed 1GeV, 6.78mA and 1mm. As shown in figure 14, maximum window temperature exceeded 870K when flow rate was $0.05\text{m}^3/\text{sec}$. Maximum window temperature decreased as increasing coolant flow rate, but maximum temperature gradient was nearly constant. Because thermal stress in window is strongly dependent on maximum temperature gradient, maximum window stress did not vary much.

3.4 Preliminary design of target and window

Based on the thermal and structural analysis, target and window design value were determined

preliminarily. Table 3-1 shows design values and operating conditions of target and window. Maximum window temperature and von-mises stress are within acceptable region. Beam power may increase more than 8mA in normal condition, not exceeding thermal and structural safety criteria.

4. Conclusion

Preliminary design and mechanical analysis of liquid Pb-Bi target and 9Cr-2WVTa window were performed. Target was designed in a way to decrease window temperature. Installation of diffuse plate which has higher porosity in central zone was considered. Temperature and stress of window were analyzed varying minimum window thickness, beam power, and coolant flow rate. Thermal-bending stress was generated in window because of temperature gradient along the thickness of window. Coolant flow rate had insignificant effect on window stresses. It can be concluded that the target and window can be used in transmutation reactor operating condition(1GeV, 6.78mA). In this study, only static analysis has been made. But, accelerator beam trip can frequently occur in accelerator operation^[5], so window and target container dynamic stress analysis will be needed. Furthermore, study about corrosion or irradiation characteristics of window will be needed in designing target and window.

References

- [1] FLUENT 4.32 User's Manual
- [2] ANSYS User's Manual for Revision 5.0
- [3] W. S. Park et al, KAERI/TR-1316/99, 1999
- [4] A. Kimura et al, "Irradiation hardening of reduced activation martensitic steels", Journal of Nuclear Materials, 233-237 (1996) 319-325.
- [5] C. Aragonese, S. Buono, et al, "A bibliographic research on the thermal fatigue of beam window structural steels", CRS4-Internal Note 01/00, 2000

Table 1. Heat generation rate in window and target (Parabolic beam)

Proton beam injection to window ($\times 10^8$ W/m³mA)

	↓	↓	↓	↓	↓	↓	↓	↓	↓	↓
10cm	9cm	8cm	7cm	6cm	5cm	4cm	3cm	2cm	1cm	
1mm	0.002	0.003	0.004	0.009	0.035	0.95	2.65	3.6	4.545	4.82

Proton beam injection to target ($\times 10^8$ W/m³mA)

	↓	↓	↓	↓	↓	↓	↓	↓	↓	↓
10cm	9cm	8cm	7cm	6cm	5cm	4cm	3cm	2cm	1cm	
10cm	0.01	0.01	0.03	0.06	0.13	0.97	2.43	3.57	4.36	4.82
10cm	0.02	0.03	0.06	0.09	0.21	0.69	1.50	2.15	2.61	2.84
10cm	0.02	0.03	0.05	0.09	0.19	0.46	0.81	1.13	1.35	1.49
10cm	0.02	0.03	0.05	0.09	0.15	0.27	0.41	0.54	0.64	0.68
10cm	0.02	0.03	0.04	0.07	0.11	0.16	0.21	0.25	0.3	0.32

Table 2. Temperature results varying diffuse plate distance

Distance between window and diffuse plate	60mm	30mm	15mm	8mm
Maximum Window Temperature	762 K	719 K	689 K	668 K
Maximum Coolant Temperature	717K	679K	663K	642K

Table 3. Preliminary target and window design value

Parameters	Values	
Target material	Pb-Bi	
Active target height	1m	
Target diameter	50cm	
Inlet flow rate	0.1m ³ /sec	
Inlet coolant temperature	613K	
Diffuse plate porosity	Zone 1	0.64
	Zone 2	0.42
	Zone 3	0.20
Distance between diffuse plate and window	8mm	
Window material	9Cr -2WV Ta	
Window diameter	30cm	
Window minimum thickness	1mm	
Beam profile	Parabolic	
Beam diameter	10cm	
Beam power	1GeV, 6.78mA	
Max. window temperature	804K	
Max. window von -mises stress	178MPa	

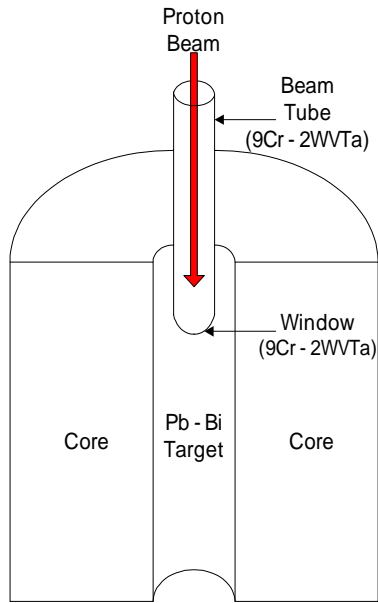


Fig 1. Subcritical reactor design

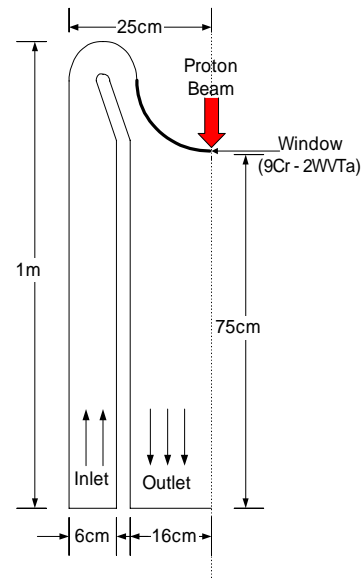


Fig 2. Target module

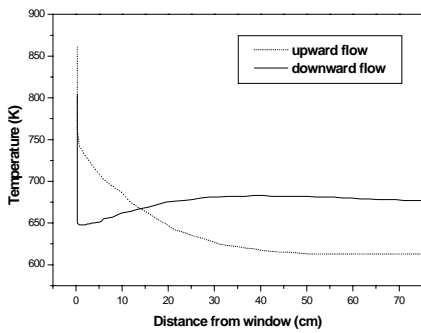


Fig 3. Effect of flow direction on temperature field

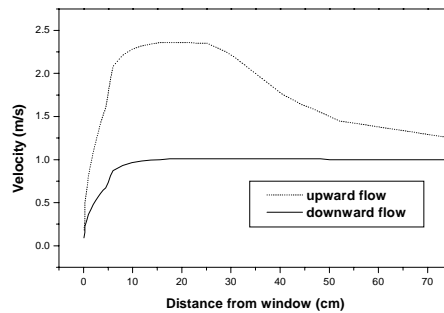


Fig 4. Effect of flow direction on velocity field

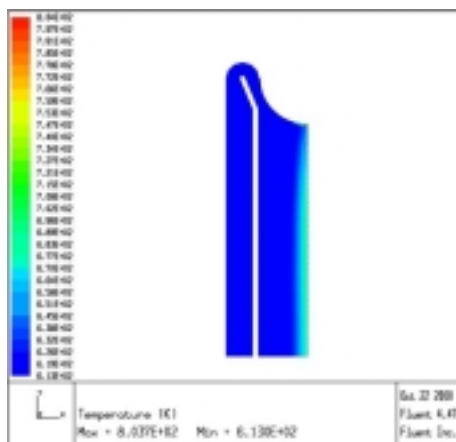


Fig 5. Temperature contours of downward flow

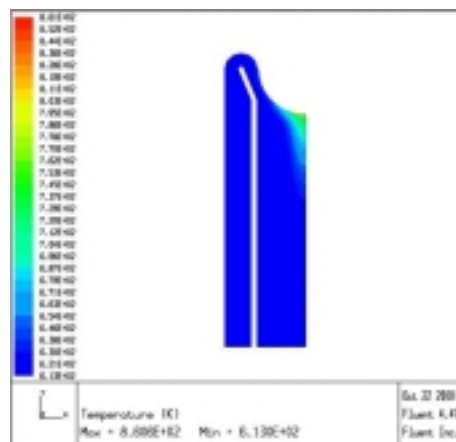


Fig 6. Temperature contours of upward flow

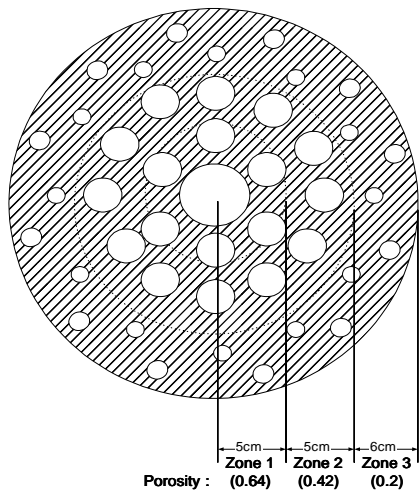


Fig 7. Diffuse plate with holes

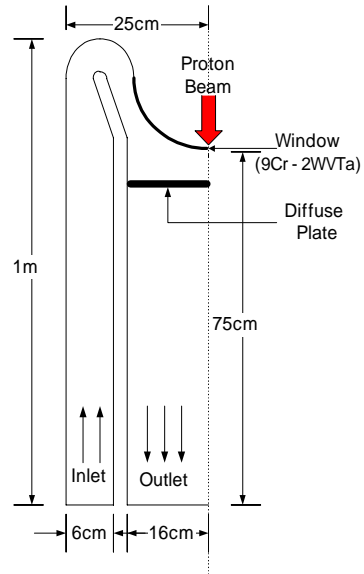


Fig 8. Target module with diffuse plate

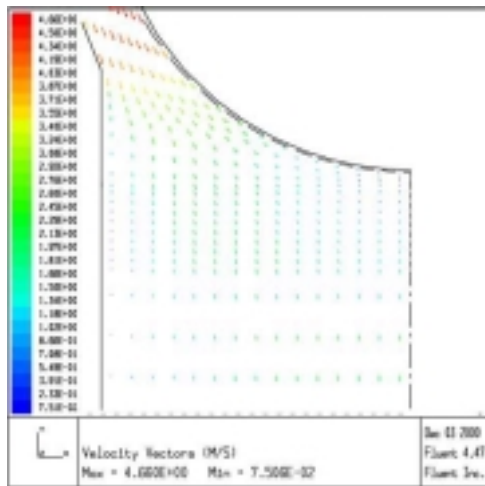


Fig 9. Velocity field without diffuse plate

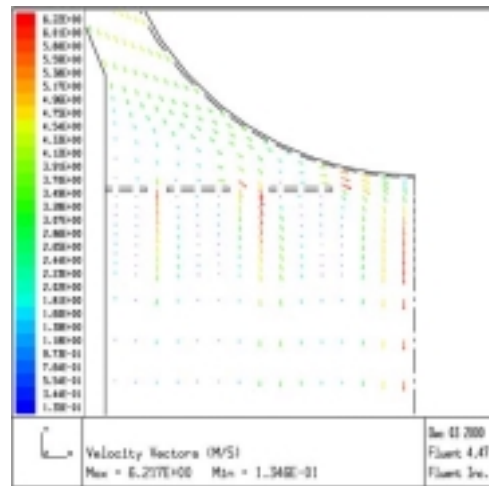


Fig 10. Velocity field with diffuse plate

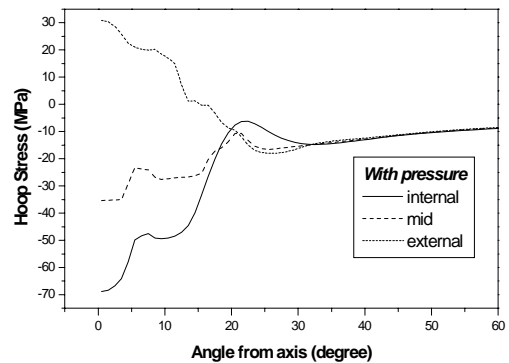
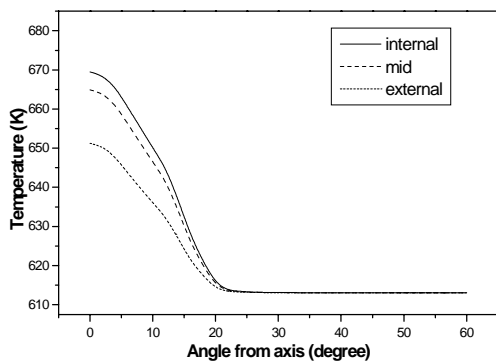


Fig 11. Window temperature and hoop stress distribution

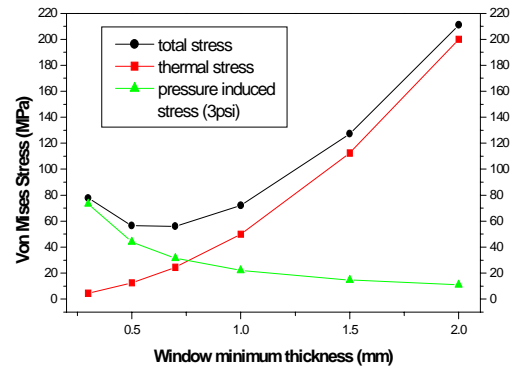
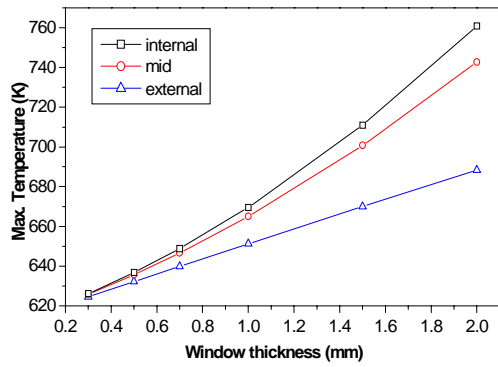


Fig 12. Effect of window thickness on maximum window temperature and stress

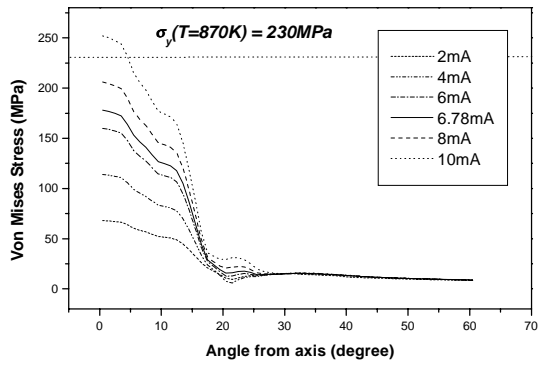
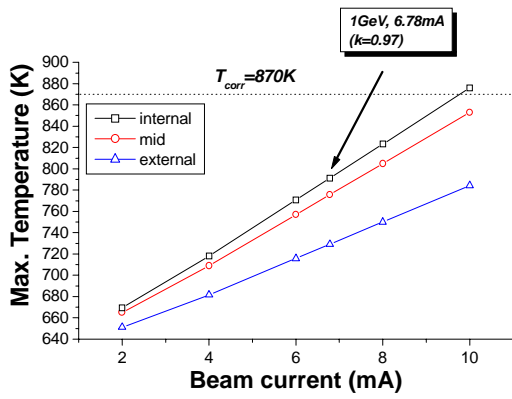


Fig 13. Effect of beam power on maximum window temperature and stress

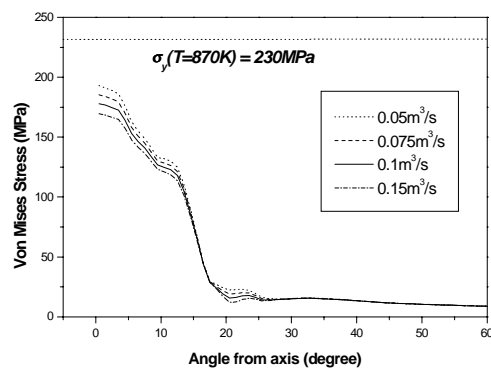
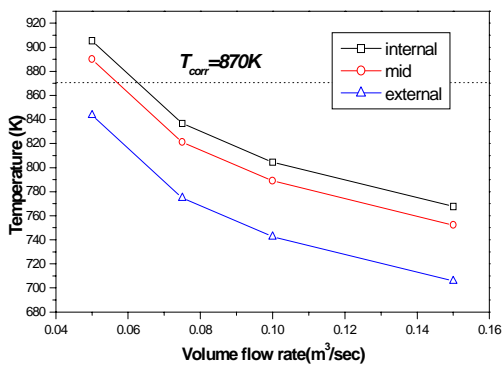


Fig 14. Effect of flow rate on maximum window temperature and stress